TABLE IV. Values of b^2 computed by the two methods suggested (Refs. 2 and 8).

Computed according to Blunck and Leisegang (Ref. 2)	Computed according to Blunck and Westphal (Ref. 8)	Ratio
40.5	34.0	1.19
8.15	6.88	1.18
4.40	3.98	1.10

lating distributions for the longer pathlengths.

VI. CONCLUSION

Although fair agreement between experiment and the Blunck-Leisegang-corrected[2] Vavilov[3] theory for the frequency distribution of small energy losses by fast charged particles in low atomic number materials has been found when the FWHM has been used for comparison, a rather poor fit results when comparisons are made over the entire range of energy losses. The discrepancies between this theory and our experimental data appear to increase as the mean energy loss for the distribution relative to the particle energy decreases.

ACKNOWLEDGMENTS

We should like to thank Professor J. R. Richardson and Dr. J. W. Verba for their cooperation in making UCLA cyclotron time available for this investigation.

*Work partially supported by NASA Grant No. NGL 05-009-103.

[1]J. W. Hilbert, N. A. Baily, and R. G. Lane, Phys. Rev. 168, 290 (1968).
[2]O. Blunck and S. Leisegang, Z. Physik 128, 500 (1950).
[3]P. V. Vavilov, Zh. Eksperim. i Teor. Fiz. 32, 320 (1957) [Soviet Phys. JETP 5, 749 (1957)].
[4]S. M. Seltzer and M. J. Berger, Natl. Acad. Sci. Natl. Res. Council, Publ. 1133, 187 (1944).
[5]U. Fano, Ann. Rev. Nucl. Sci. 13, 1 (1963).
[6]W. Börsch-Supan, J. Res. Natl. Bur. Std. (U. S.), 65B, 245 (1961).
[7]L. Landau, J. Phys. USSR 8, 201 (1944).
[8]O. Blunck and K. Westphal, Z. Physik 130, 641 (1951).
[9]J. L. Campbell and D. K. Ledingham, Brit. J. Appl. Phys. 17, 769 (1966).
[10]H. D. Maccabee, M. R. Raju, and C. A. Tobias, Phys. Rev. 165, 469 (1968).
[11]H. Bichsel, Phys. Rev. B 1, 2854 (1970).

PHYSICAL REVIEW B VOLUME 2, NUMBER 3 1 AUGUST 1970

Fast-Electron Channeling Investigated by Means of Rutherford Scattering

E. Uggerhøj and F. Frandsen

Institute of Physics, University of Aarhus, 8000 *Aarhus* C, *Denmark*

(Received 10 December 1969)

The Rutherford-scattering and transmission yields for electrons incident on thin single crystals have been measured. For the Rutherford-scattering yield, very pronounced peaks are found whenever the incoming beam is incident on the crystal within a certain critical angle of a low-index direction. The full width at half-maximum for the peak in yield is found to be proportional to Ψ_1, the Lindhard critical angle. Also, the volume of the peak is found to be conserved for gold crystals of thicknesses up to around 5000 Å. Further, experimental investigations of the multiple scattering for single crystals and polycrystalline foils are discussed.

INTRODUCTION

In the past few years, the influence of lattice structure on the motion of heavy charged particles in crystals has been widely investigated (for a review, see Ref. 1). It has been shown that the experimental results are in good agreement with Lindhard's theory[2] derived from classical orbital mechanics. It has also been shown that these directional effects are powerful tools for the localization of foreign atoms in single crystals and for measurements of radiation damage in single crystals and its annealing behavior. Until now, investigations of directional effects by means of light

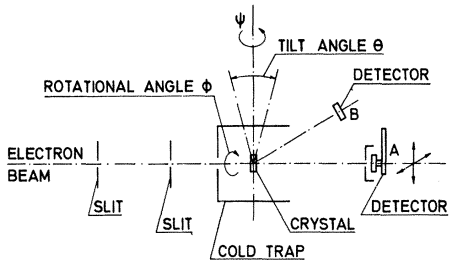

FIG. 1. Schematic drawing of the experimental setup.

charged particles (i.e., electrons and positrons) have mostly been performed by measuring the emission of electrons and positrons from radioactive nuclei embedded in single crystals.[3] It was found that the positrons, on the one hand, show very pronounced dips in yield whenever they are emitted within a critical angle around an axial or planar direction. As shown by Lervig *et al.*,[4] the positrons are expected to behave nearly classically, and the full widths at half-minimum of the dip in emission yield may be compared with the Lindhard estimate of the critical angle. A more detailed discussion of these aspects is given in the paper by Andersen *et al.*[5] Conversely, for electrons, a very pronounced peak in yield was found when the emission direction was within a certain critical angle around an axial or planar direction.

In the above-mentioned emission experiments, radiation damage was created in the single crystal due to the fact that the total dose implanted into the crystal was relatively large ($\sim 5\times 10^{14}$ ions/cm^2). Therefore, the experimental results are somewhat uncertain.

A more precise way of investigating such effects may be to inject an external electron or positron beam and measure wide-angle Rutherford scattering. The only disadvantage, as compared to the above, is that thin foils will be needed in order to have well-defined depths. The present paper describes some experimental investigations of the influence of crystal structure on wide-angle Rutherford scattering of electrons incident on a thin single crystal. Some investigations of the multiple scattering of electrons traversing thin foils (polycrystalline and crystalline) are reported.

EXPERIMENTAL PROCEDURE

Figure 1 shows the experimental setup. A beam of electrons is obtained from the 2-MV Van de Graaff at Aarhus. By the slit system, the half-angular spread of the beam is reduced to 0.05°. In Figs. 2–7, however, the spread of the beam is 0.1°.

The thin single crystals were mounted in a goniometer with a 360° rotation axis (φ) and two perpendicular axes (ψ and θ). The goniometer is provided with step motors by which the angle reading is accurate to within 0.01°.

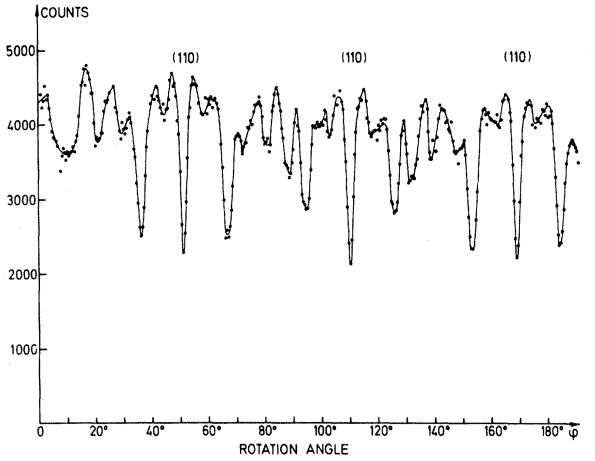

FIG. 2. Orientation dependence of the electrons transmitted in the forward direction. The scan is a rotation around the [111] axis with the tilt angle θ held at 15°. Electron energy: 1 MeV. The crystal thickness was around 300 Å.

In the present experiment, two solid-state Si detectors (A and B) were mounted. From the energy spectra of the detectors, the electron spectra were easily resolved from the γ background. Electrons transmitted in the forward direction were counted by detector A, a Li-drifted surface-barrier detector with a 3-mm-thick depletion layer. By means of step motors, this detector can be moved vertically and horizontally, thus enabling the multiple scattering to be measured.

In the Rutherford-scattering experiments, it is possible to align either the incoming or the outgoing electrons with major directions in the crystal. We have chosen to align the incoming elec-

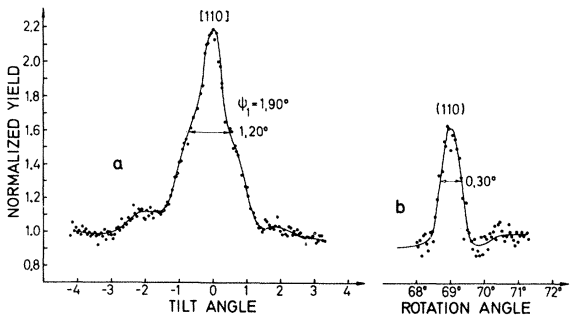

FIG. 3. Normalized scattering yield of 1-MeV electrons incident upon a [111] gold crystal. Crystal thickness: 1200 Å. (a) [110] axis. (b) (110) plane. Here the tilt angle is kept constant at 25°.

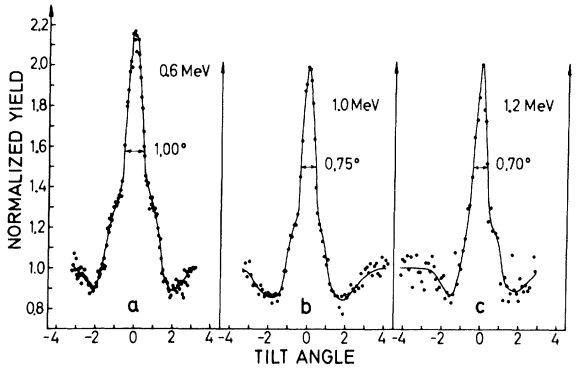

FIG. 4. Energy dependence of Rutherford-scattering yield for electrons incident along the [111] axis in a gold crystal. Crystal thickness: 600 Å.

trons with axial or planar directions. To avoid the complication of accidentally aligning the outgoing path with a crystal direction, a large (80 mm^2) detector (B) averaging over many crystal directions was used. Detector B was made by ion implantation and had a 2-mm-thick depletion layer. The scattering angle in all the present experiments was from 15° to 25°. The total energy loss for the electrons in the present investigations was negligible since it was only around 1 keV for the thicker foils.

Crystal Preparation

Thin gold crystals of thicknesses ranging from ~600 to ~4000 Å were epitaxially grown by Ambrosius-Olesen. The general technique used was the same as that described by Gibson *et al.*,[6] combined with a "pulsed" evaporation technique outlined by Chadderton and Andersen.[7]

Only crystals displaying (i) good electron diffraction patterns, (ii) undisturbed and unwrinkled surfaces, and (iii) very pronounced dips in Rutherford-scattering yield of protons were used in these experiments.

First, a precise orientation of the crystal was obtained by measuring the number of electrons transmitted in the forward direction for different rotation angles. Figure 2 shows the variation in transmission yield when the crystal is rotated around an axis at a tilt angle of 15° to the [111] direction. It is observed that whenever the incoming beam is aligned with close-packed planes, a large fraction of the beam is scattered into diffracted beams, thus causing a pronounced and sharp dip in transmission yield. From these dips, the orientation is easily found within 0.05° or better. Further, it is possible to investigate the crystal for twinning, as this will change the rotation scan around the [111] axis (for a large tilt angle) from a threefold to a sixfold symmetry. This technique for orientation provides a fast and accurate method of alignment.

RESULTS

Figures 3–7 show the yields normalized to the average yield in a random direction.

Figure 3 shows the wide-angle Rutherford-scattering yield as a function of the angle between the beam direction and either a string (a) or a planar (b) direction. The electron energy is 1 MeV, and the crystal thickness ~1200 Å. In the string case, the scattering yield displays a peak up to 2.2 times normal yield. The small "humps" for $\theta = \pm 0.8°$ and $\pm 2.0°$ are presumably due to the circumstance that some planar effects are involved, since it is very difficult to tilt through a crystal axis without having any influence of the planar channeling. This assumption is fortified by the fact that there are small humps on some of the curves in Figs. 3–7, but not on other curves, and also that such humps do not seem to occur on planar scans. To some extent, the existence of these humps may, of course, influence the full widths at half-maximum of the peaks. Until detailed investigations of the influence of planar effects, mosaic spread, and radiation damage on the full widths of the peaks have been performed, these perturbations are disregarded. The influence of the humps on the volume of the peaks is discussed below. The crystal was tested by wide-angle Rutherford scattering of 400-keV protons, giving a dip in yield down to approximately 4% of normal yield, thus indicating that the crystal is rather perfect. Figure 3(b) shows that the planes have a similar steering effect as the string. This circumstance gives rise to a peak in electron scattering yield of around 60% over normal yield.

Figures 4 and 5 show investigations of the full width at half-maximum in the scattering yield when the energy and the distance d between atoms in the

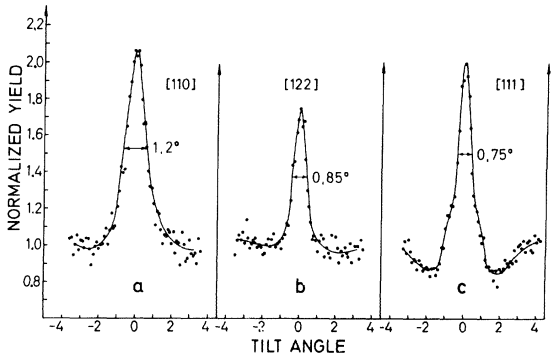

FIG. 5. Variation of the Rutherford-scattering yield for 1-MeV electrons as a function of direction in a gold crystal. Crystal thickness: 600 Å.

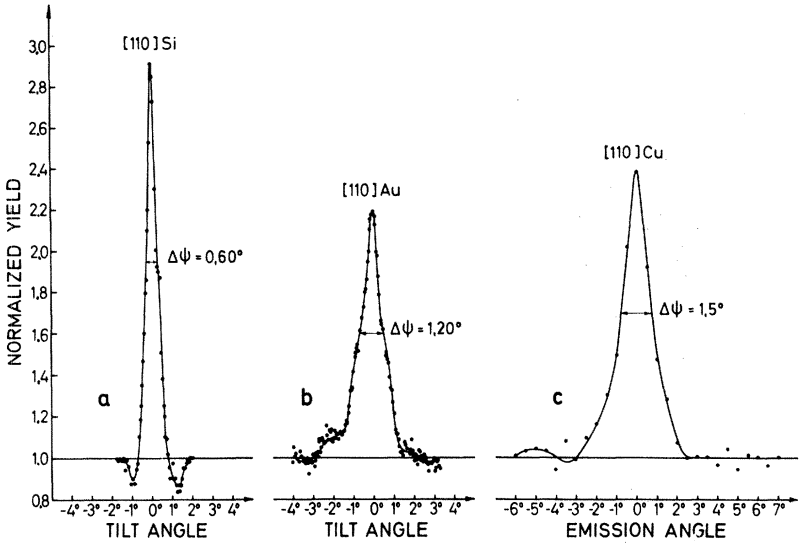

FIG. 6. Variation of the full width at half-maximum ($\Delta\psi$) as a function of target material.

atomic row are varied. The crystal was 600 Å thick, but was not as perfect as the thicker crystal, since the minimum dip in yield for wide-angle Rutherford scattering of protons was as high as 10% of the normal yield. The variation in d was obtained by tilting the crystal to several low-index directions. The peak height for the [121] axis in Fig. 5 is approximately 20% lower than that for other directions. The distance between the atoms in this row is smaller than that of the atoms in the [111] axis, so a lower peak height for the [121] axis would not be expected. This may, however, be due to the fact that the tilt plane is slightly off the [121] center.

Figure 6(a) is the same as Fig. 3(a), and Fig. 6(b) shows the variation in Rutherford-scattering yield (scattering angle: 15°–25°) of 600-keV electrons incident along the [110] axis in a 300-Å-thick Si crystal. The measurements on Si were performed by Andersen and co-workers at Bell Telephone Laboratories, N. J. Figure 6(c) shows the variation in electron emission yield around the [110] axis in Cu. The energies varied from 370 to 445 keV. (The curve was taken from Ref. 3.)

Figures 7(a)–7(d) show some preliminary results of the variation in Rutherford-scattering yield for 1-MeV electrons incident on [110] Au crystals of different thicknesses. For protons, the three crystals in Figs. 7(b)–7(d) have shown dips in Rutherford-scattering yield down to about 4% (or less) of normal yield, so the crystals are rather perfect, whereas Fig. 7(a) only showed a dip in yield down to 10%.

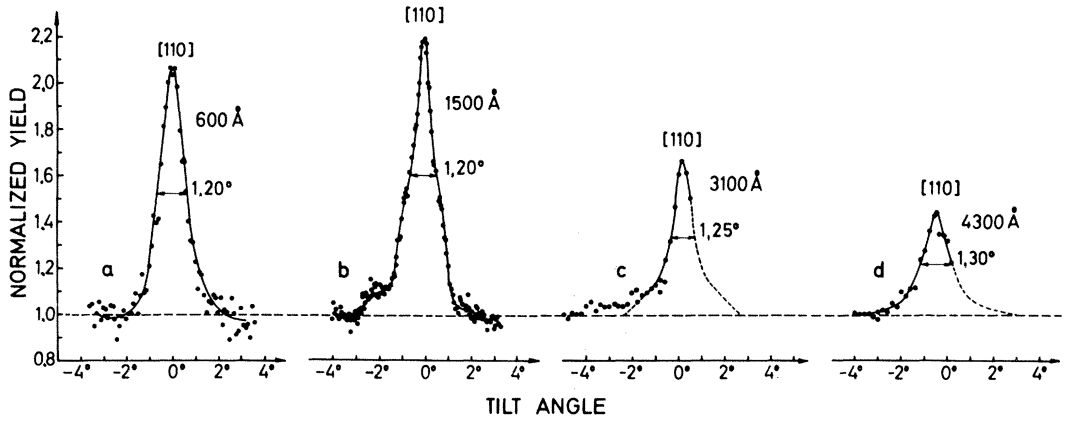

FIG. 7. Variation of the Rutherford-scattering yield for 1-MeV electrons incident on gold crystals of different thicknesses.

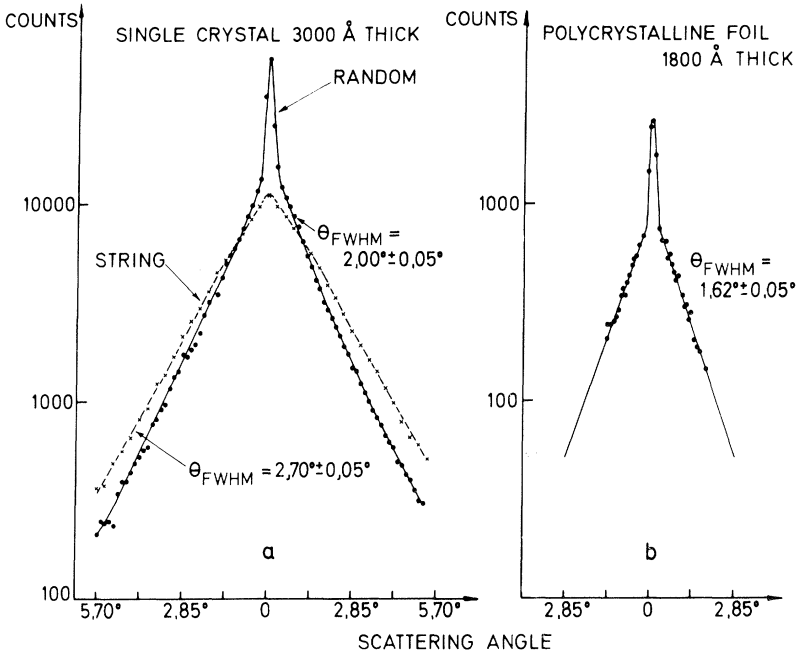

FIG. 8. Angular distribution of the electrons after transmission through a 3000-Å gold crystal (a) and a 1800-Å-thick polycrystalline foil (b).

Figure 8(b) shows the multiple scattering of 1-MeV electrons traversing an 1800-Å-thick polycrystalline gold foil. Angular distributions of the electrons transmitted through a 3000-Å-thick single crystal are shown in Fig. 8(a) for a random and a string direction. It is seen that the distribution consists of a narrow middle peak with a full width at half-maximum equal to the beam divergence, i.e., that the total scattering angle of the electrons in the peak was, at most, equal to the beam divergence. From the volume of the peak, the mean number of scattering events is obtained. In the string case, the middle peak has disappeared, indicating that the mean number of scattering events has increased. The broad distributions are the multiple (plural) and single scattering distributions. The multiple scattering angle squared Ω^2 is increased by approximately 20% when tilting from a random to a string direction.

DISCUSSION

In the early emission experiments,[3] the full widths at half-minimum of the dips for positrons were found to be in good agreement with Lindhard's critical angle ψ_1, found from the classical description, where

$$\psi_1 \simeq (2Z_1Z_2e^2/d \times \tfrac{1}{2}pv)^{1/2} . \quad (1)$$

Here, Z_1 and Z_2 are the atomic numbers of the projectile and the target, respectively, e the charge of the electron, d the distance between atoms in a row, and p and v the relativistic momentum and velocity, respectively. A more detailed discussion of whether or not it is reasonable to use a classical description for positrons is given in Ref. 4.

For electrons, the question is whether or not the present results should be compared with classical calculations. In the Lindhard paper,[8] the quantities that discern between a classical and a quantum-mechanical description are discussed. It is pointed out that whenever the number ν of bound states in the transverse phase space is large, the classical approximation is favorable. For electrons, the number of bound states ν_s in the string potential is given by

$$\nu_s = (1/\hbar^2) \int\int d^2r d^2p_\perp \big|_{E_\perp \leq 0} ,$$

where $E_\perp = p_\perp^2/2m + U(r)$, $p_\perp$ being the transverse momentum and m the relativistic mass.

By using the standard potential (see Ref. 2) for $U(r)$, it is found that

$$\nu_s \simeq \frac{1}{(1-v^2/c^2)^{1/2}} Z_2^{1/3} \frac{4a_0}{d} .$$

By using the planar potential (Ref. 2) instead of the standard potential, the number ν_p of bound states in the planar potential is found to be

$$\nu_p \simeq \frac{0.4}{(1-v^2/c^2)^{1/4}}$$

in the case where the distance between planes, d_p, is equal to $5a_0$. Here, v and c are the velocities of the electron and light, respectively, Z_2 the atomic number of the target, a_0 the Bohr radius, and d the distance between atoms in a row. For

1-MeV electrons on a gold crystal, $\nu_s \simeq 10$ and $\nu_p \lesssim 1$, showing that for the string case it is reasonable to compare the experimental results with a classical calculation, whereas the results for the planes have to be compared with a quantum-mechanical calculation.

String Effect

Figure 3(a) shows that whenever the electron beam is aligned with an axial direction, there is an increased probability of hitting the nuclei in the string, which gives rise to a peak in the Rutherford-scattering yield. The observed peak gives the increase in yield averaged over all depths in the crystal, because the energy resolution of the detector corresponds to a depth resolution of about 5 μ. In the present case, the average peak is about 120% over normal yield, but the peak height is sensitive to imperfections in the crystal and to multiple scattering.

In the Lindhard paper,[8] a formula is given for the distribution I_p of the excess of Rutherford-scattering yield as a function of the angle ψ between the beam direction and an axis direction. For such small depths, where multiple scattering can be disregarded, it is found that

$$I_p(\psi) \simeq e^{-2\psi^2/\psi_1^2} \ln(\alpha\gamma) \quad \text{for} \quad \alpha \gg 1, \tag{2}$$

where ψ_1 is the critical angle, $\gamma = 1.78$ the Euler constant, $\alpha = C^2 a^2/\rho^2$ with $C^2 \simeq 3$, a the Thomas-Fermi screening distance, and ρ^2 the mean square thermal vibrational amplitude. For negative particles, the compensation (I_c) for I_p appears as a shallow dip stretching from $\psi = 0$ out to angles somewhat larger than Ca/d, d being the distance between atoms in the row. The integral of $I(\psi) = I_p(\psi) + I_c(\psi)$ over all angles is zero.

Because of the rule of reversibility (cf. Ref. 2), the distribution in Rutherford-scattering yield from an external electron beam is identical to the distribution of electrons emitted from lattice sites. For the emission case, the integrated extra yield, e.g.,

$$\omega = \int I_p(\psi) 2\pi\psi d\psi = (\pi\psi_1^2/2) \ln(\gamma\alpha), \quad \alpha \gg 1 \tag{3}$$

represents the number of electrons emitted with $E_\perp < 0$ relative to the number of emitted particles per solid angle in the random case. As the number of particles originally emitted with $E_\perp < 0$ is independent of depth, the integrated extra yield must be the same for all depths. However, a calculation of the angular distribution $I_p(\psi)$ as a function of depth is not simple because it requires detailed knowledge of the multiple scattering for the string case.

It follows from the above that the peak volume ω is conserved as long as the influence of I_c is negligible. This is the case until such depths are reached that multiple scattering has broadened out the peak to angles of the order of Ca/d.

In our case, where Au was used, a comparison with the above formula is not favorable since ρ^2 is large (~ 0.023 Å) and a is small (~ 0.11 Å), whereby $\alpha \approx 1.5$. For the present case, a reasonable estimate shows that a positive correction term has to be added to the asymptotic expression for ω. In the gold case, this correction may amount to around 40% of the log term. For a more detailed description, see Ref. 9.

For 1-MeV electrons incident along the [110] axis in gold, the corrected volume ω is ~ 8.5 (deg^2). The integrated volume of the peak in Fig. 3(a) is found to be $\simeq 2.3$ (deg^2). In the present case, the negative compensation will lower somewhat the value of ω since the critical angle ($\psi_1 = 1.9°$) is approximately half the width of the negative compensation ($a/d \approx 4.2°$). Yet, the theoretical value still appears to be significantly larger than the experimental value. The same trend appears from the Si and Cu data shown in Fig. 6. In the evaluation of the peak volumes, the volume of the "humps" has been neglected on the assumption that these humps are due to planar effects and that a two-dimentional scan around an axis would show similar dips. Thereby the total contribution to the peak volume from all planar effects has been set equal to zero. The experimental values are also somewhat sensitive to how the random level is placed.

It should be mentioned that the discrepancy between the theoretical and the experimental volume is due to the circumstance that all the experimental peaks in Fig. 6 are narrower than the theoretical ones [formula (2)], whereas the experimental peak heights are practically equal to those found theoretically (the log terms).

As mentioned above, the peak volume is approximately constant until such depths where the multiple scattering width Ω is comparable with Ca/d. In the present case, $Ca/d \approx 4.2°$, and Fig. 8 shows that the multiple scattering for the [110] axis in a 3000-Å-thick Au crystal is around 1.35°. So, the peak volume should be conserved for thicknesses less than 4–5000 Å, which is in fairly good agreement with the experimental results shown in Fig. 7, where the volumes are Fig. 7(a): 2.1, Fig. 7(b): 2.2, and Fig. 7(d): 1.9; the volume of Fig. 7(c) is somewhat uncertain because of planar effects causing the long "tail" on the peak. If this tail is disregarded, the volume is about 2.5. Thus, the over-all conservation of the peak volume is good.

In Tables I and II are summarized the experimental results shown in Figs. 4 and 5 in order to point out that the half-width at half-maximum ($\Delta\psi$)

TABLE I. Comparison between ψ_1 and the $\Delta\psi$ values for electrons of different energies incident along the [111] axis in a gold crystal.

Electron energy	0.6 MeV	1.0 MeV	1.2 MeV
$\Delta\psi$	$1.00°\pm0.05°$	$0.75°\pm0.05°$	$0.70°\pm0.05°$
$\Delta\psi/\psi_1$	0.66	0.63	0.64

for the Rutherford-scattering peak is proportional to ψ_1 as long as the central peak is not smeared out by multiple scattering. It is seen that $\Delta\psi$ is proportional to ψ_1 with a factor of proportionality of about 0.6.

With respect to the Z_2 dependence of the $\Delta\psi$ values, only very few experimental results are yet available. Table III summarizes the results from Fig. 6, and the experimental values are compared with the calculated ψ_1 values. It is seen that the factor of proportionality between the measured $\Delta\psi$ values and the theoretical ψ_1 values is somewhat changing. But when $\Delta\psi$ and ψ_1 values for different crystals are compared, the Debye temperature for the three crystals varies from 162 (Au) to 580 °K (Si). Therefore the influence of thermal vibrations on the $\Delta\psi$ values changes. For a more detailed investigation of the influence of temperature on $\Delta\psi$ for positive particles, see Ref. 11.

Further, regarding the wide-angle Rutherford scattering of protons, it is known that if the half-widths at half-minimum ($\Delta\psi_{H+}$) for the dips in yield are compared with theoretical ψ_1 values, the factor of proportionality is also somewhat changing from element to element. Therefore Table III also shows the $\Delta\psi_{H+}$ values taken from wide-angle Rutherford scattering of protons on the same crystals. Concerning the proton energies used in these cases, 1-MeV electrons are compared with ~670-keV protons since $\frac{1}{2}pv$ enters in formula (1) rather than the kinetic energy E. It is seen that within experimental error, $\Delta\psi=\frac{1}{2}\Delta\psi_{H+}$. This is in agreement with qualitative classical calculations based on the continuum approximation; see Ref. 3. However, it should be pointed out that this comparison between the $\Delta\psi$ values and the ψ_1 values is not quite

TABLE II. Comparison between ψ_1 and $\Delta\psi$ values for 1-MeV electrons incident along different directions in a gold crystal.

Crystal direction	[110]	[121]	[111]
$\Delta\psi$	$1.20°\pm0.05°$	$0.85°\pm0.05°$	$0.75°\pm0.05°$
$\Delta\psi/\psi_1$	0.63	0.61	0.63

TABLE III. Comparison between $\Delta\psi$, ψ_1, and $\frac{1}{2}\Delta\psi_{H+}$ for various crystals.

Crystal (electron energy)	Au (1 MeV)		Cu (405 keV)	Si (600 keV)
Axis	[110]	[111]	[110]	[110]
$\Delta\psi$	$1.20°\pm0.05°$	$0.75°\pm0.05°$	$1.5°\pm0.1°$	0.60°
ψ_1	1.9°	1.2°	1.8°	0.85°
$\frac{1}{2}\Delta\psi_{H+}$	$1.3°\pm0.1°$	$0.8°\pm0.1°$	$1.4°\pm0.1°$	0.65°[a]

[a]Taken from Ref. 10.

justified in the Cu and Si cases because the energies are too low to give a large number of quantum states in phase space.

Planar Effects

As shown above, the number of quantum states in phase space for the planes is smaller than unity; this means that the experimental results should be compared with quantum-mechanical calculations, for example, of the type outlined by DeWames *et al.*[12] In Fig. 9, the experimental results from Fig. 3(b) are compared with a nine- and a thirteen-beam calculation. (The program for this calculation has been made by Andersen.) It is seen that the calculated full width at half-maximum is in fairly good agreement with the experimental results, whereas the calculated peak height is much larger than the experimental one, but the calculations are made for very thin crystals. In another calculation, a Debye-Waller factor was introduced into the nine-beam calculation, but with no noteworthy change in the result.

Multiple Scattering

From Rutherford-scattering results it is seen that electrons in a beam aligned with a string (or planar) direction have an increased probability of hitting the nuclei in a string (plane). Consequently, the multiple scattering of these electrons is larger than normal, as seen in Fig. 8. In order to clear up the multiple scattering of electrons on very thin polycrystalline foils, a number of experimental investigations have been performed and will be published elsewhere. From the volume of the unscattered peak it is found that a foil thickness of about 400 Å on the average corresponds to one scattering event. If the distribution of the electrons outside the unscattered part is regarded as consisting of a Gaussian (multiple scattering) and a "tail" (single scattering), then for foils of thicknesses $\gtrsim$3000 Å, the spread in the Gaussian agrees well with the values obtained from the Moliere[13] theory. For very thin foils, the distributions are in good agreement with those calculated by Keil *et al.*[14] According to the Moliere theory, the full

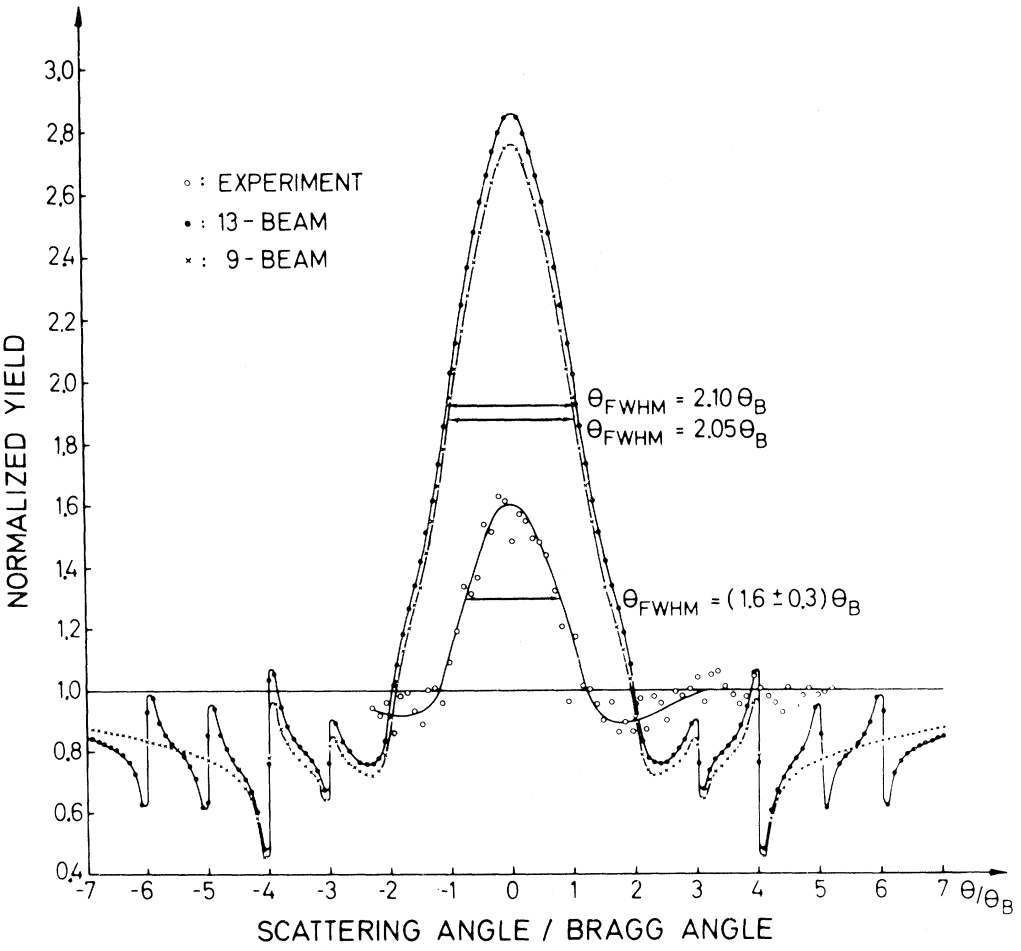

FIG. 9. Comparison between the electron peak in Fig. 3(b) and the distribution in scattering yield obtained from a nine- and a thirteen-beam calculation.

width at half-maximum for a 3000-Å-thick gold foil is 2.0°; this is in good agreement with the experimental results.

CONCLUSIONS

For 1-MeV electrons in gold, the experimental results for the string case are in good agreement with a classical calculation. These results are consistent with the criterion given by Lindhard[8] for the validity of the classical treatment, viz., that the number of bound states in phase space has to be much larger than unity.

ACKNOWLEDGMENTS

We are much indebted to J. U. Andersen, E. Bonderup, J. Lindhard, and K. O. Nielsen for fruitful discussions. It is also a pleasure to thank J. Bøttiger, who took part in some of the experiments, and P. Ambrosius-Olesen, who made the gold crystals.

[1]S. Datz, C. Erginsoy, G. Leibfried, and H. O. Lutz, Ann. Rev. Nucl. Sci. 17, 129 (1967).

[2]J. Lindhard, Kgl. Danske Videnskab. Selskab, Mat.-Fys. Medd. 34, No. 14 (1965).

[3]E. Uggerhøj and J. U. Andersen, Can. J. Phys. 46, 543 (1968).

[4]P. Lervig, J. Lindhard, and V. Nielsen, Nucl. Phys. A96, 481 (1967).

[5]J. U. Andersen, W. M. Augustinyak, and E. Uggerhøj (unpublished).

[6]W. M. Gibson, J. B. Rasmussen, P. Ambrosius-Olesen, and C. J. Andreen, Can. J. Phys. 46, 551 (1968).

[7]L. Chadderton and M. Andersen, Thin Films 1, 229 (1969).

[8]J. Lindhard, in *Atomic Collision Phenomena in Solids*

(North-Holland, Amsterdam, 1970), Chap. 1.
[9]E. Bonderup and J. Lindhard, Kgl. Danske Videnskab. Selskab, Mat.-Fys. Medd. (to be published).
[10]S. T. Picraux, J. A. Davies, L. Eriksson, N. G. E. Johansson, and J. W. Mayer, Phys. Rev. 180, 873 (1969).
[11]J. U. Andersen and E. Uggerhøj, Can. J. Phys. 46, 517 (1968).
[12]R. E. DeWames, W. F. Hall, and L. T. Chadderton, in Proceedings of the International Conference on Solid State Physics, Research with Accelerators, Brookhaven, 1967 (unpublished).
[13]G. Moliere, Z. Naturforsch. 3a, 78 (1948).
[14]E. Keil, E. Zeitler, and W. Zinn, Z. Naturforsch. 15a, 1031 (1960).

PHYSICAL REVIEW B VOLUME 2, NUMBER 3 1 AUGUST 1970

No-Phonon ^4T_2g - ^4A_2g Transitions of Cr^{3+} in TiO_2

Ludwig Grabner, S. E. Stokowski, *† and W. S. Brower, Jr.
National Bureau of Standards, Washington, D.C. 20234
(Received 17 March 1970)

Absorption and emission at 4 and 77 K are observed in Cr-doped TiO_2 consisting of two sharp no-phonon lines at 12 685 and 12 732 cm^{-1}, and vibronic sidebands with an integrated intensity 10^4 times that of the no-phonon lines. In undoped TiO_2, identical spectra are observed but are a factor of 100 less intense. The center responsible for these spectra is identified as substitutional Cr^{3+} by observing, in emission, a splitting of the 12 685-cm^{-1} line of 1.4 cm^{-1}, a value previously determined by EPR measurements. The vibronic sidebands have some structure superposed on a broad band. The vibronics are different in emission and absorption and have a lifetime of 45 μsec, equal to that of the no-phonon line. They are shown to be principally due to defect-induced phonons arising from the Cr^{3+} defect. We argue that the spectra observed are not characteristic of the usual ^2E_g-$^4A_{2g}$ transition, and propose that the $^4T_2$ lies lower in energy than the ^2E_g state. If so, the new results of this work are (1) no-phonon line emission for the $^4T_2$-$^4A_2$ transition and (2) defect phonon states which are different for the $^4A_2$ and $^4T_2$ states. The excitation spectrum is also presented. It shows that the excitation of the Cr^{3+} emission occurs mainly by the transfer of energy from excited trapping centers rather than by direct excitation.

I. INTRODUCTION

The motivation for the experiments to be reported in this paper was the observation, upon preliminary examination at 77 K, of sharp line photoluminescence at ~8000 Å in undoped TiO_2. In some ways, the fluorescence suggested similarities to that of Cr^{3+} in $SrTiO_3$ in which one of us[1] (S.S.) suggested that it is due to Cr^{3+} while the other[2] (L.G.) proposed that it is not. Later, Burke and Pressley[3] in a study of the Zeeman effect of the sharp line infrared fluorescence of $SrTiO_3$ concluded that the sharp line could be consistently interpreted as a transition from the ^2E_g state to the $^4A_{2g}$ state of Cr^{3+}. The question then arose: is the fluorescence observed in undoped TiO_2 due to a Cr^{3+} ion or not? This decision was facilitated by the study of Gerritsen *et al.*[4] of the electron paramagnetic resonance spectrum of Cr-doped TiO_2 in which the splitting of the $^4A_{2g}$ ground state of Cr^{3+} was measured to be 1.4 cm^{-1} and, therefore, easily resolved optically. In brief then, optical absorption, photoluminescence, and excitation spectra presented in this paper unequivocally decide in favor of Cr^{3+} fluorescence in TiO_2. Thus, just as in the case of $SrTiO_3$, spectrochemically undetectable amounts of Cr are easily detected in photoluminescence.

However, analysis of our data presented unexpected difficulties for the "standard" interpretation in which the lowest-lying electronic excited state of the Cr^{3+} is the ^2E_g state. Instead we believe that our data suggest that the $^4T_{2g}$ state is the lowest-lying electronic excited state of Cr^{3+} in TiO_2, and a major portion of this paper is devoted to this thesis. If our suggestion is correct, the $^4T_{2g} \rightarrow {}^4A_{2g}$ emission of Cr^{3+} in TiO_2 is unique in that this transition gives rise to *line emission* in addition to the usual broad-band emission. Previous work on Cr^{3+} in octahedral oxygen coordination show only a few cases[5-7] in which the lowest excited state is the $^4T_{2g}$ state rather than the ^2E_g state. In contrast to Cr^{3+} in TiO_2, however, the $^4T_{2g}$ zero-phonon transition was not seen.